



HAL
open science

Long-term seismicity of the Reykjanes Ridge (North Atlantic) recorded by a regional hydrophone array.

Jean Goslin, N. Lourenco, R. P. Dziak, D.R. Bohnenstiehl, J. Haxel, J. Luis

► To cite this version:

Jean Goslin, N. Lourenco, R. P. Dziak, D.R. Bohnenstiehl, J. Haxel, et al.. Long-term seismicity of the Reykjanes Ridge (North Atlantic) recorded by a regional hydrophone array.. *Geophysical Journal International*, 2005, 162 (2), pp.516-524. 10.1111/j.1365-246X.2005.02678.x . hal-00112614

HAL Id: hal-00112614

<https://hal.science/hal-00112614>

Submitted on 19 Feb 2021

HAL is a multi-disciplinary open access archive for the deposit and dissemination of scientific research documents, whether they are published or not. The documents may come from teaching and research institutions in France or abroad, or from public or private research centers.

L'archive ouverte pluridisciplinaire **HAL**, est destinée au dépôt et à la diffusion de documents scientifiques de niveau recherche, publiés ou non, émanant des établissements d'enseignement et de recherche français ou étrangers, des laboratoires publics ou privés.

Long-term seismicity of the Reykjanes Ridge (North Atlantic) recorded by a regional hydrophone array

Jean Goslin,¹ Nuno Lourenço,^{2,3} Robert P. Dziak,⁴ DelWayne R. Bohnenstiehl,⁵ Joe Haxel³ and Joaquim Luis²

¹UMR CNRS 6538, Institut Universitaire Européen de la Mer, Université de Bretagne Occidentale, Technopôle Brest Iroise, 29280 Plouzané, France.

E-mail: goslin@univ-brest.fr (JG)

²Centro de Investigação Marinha e Ambiental, Universidade do Algarve, Campus de Gambelas, 8000 Faro, Portugal. E-mails: lourenco@fc.ul.pt (NL);

jluis@ualg.pt (JL)

³Centro de Geofísica de Universidade de Lisboa, Campo Grande, 1749-016 Lisboa, Portugal

⁴Pacific Marine Environmental Laboratory, Oregon State University/NOAA, Marine Hatfield Center, Newport, Oregon, USA.

E-mails: robert.p.dziak@noaa.gov (RPD); joe.haxel@noaa.gov (JH)

⁵Lamont Doherty Earth Observatory of Columbia University, Palisades, New York, USA. E-mail: del@ldeo.columbia.edu (DRB)

Accepted 2005 May 9. Received 2005 May 4; in original form 2004 November 9

SUMMARY

The seismicity of the northern Mid-Atlantic Ridge was recorded by two hydrophone networks moored in the sound fixing and ranging (SOFAR) channel, on the flanks of the Mid-Atlantic Ridge, north and south of the Azores. During its period of operation (05/2002–09/2003), the northern ‘SIRENA’ network, deployed between latitudes 40° 20′N and 50° 30′N, recorded acoustic signals generated by 809 earthquakes on the hotspot-influenced Reykjanes Ridge. This activity was distributed between five spatio-temporal event clusters, each initiated by a moderate-to-large magnitude (4.0–5.6 M) earthquake. The rate of earthquake occurrence within the initial portion of the largest sequence (which began on 2002 October 6) is described adequately by a modified Omori law aftershock model. Although this is consistent with triggering by tectonic processes, none of the Reykjanes Ridge sequences are dominated by a single large-magnitude earthquake, and they appear to be of relatively short duration (0.35–4.5 d) when compared to previously described mid-ocean ridge aftershock sequences. The occurrence of several near-equal magnitude events distributed throughout each sequence is inconsistent with the simple relaxation of mainshock-induced stresses and may reflect the involvement of magmatic or fluid processes along this deep (>2000 m) section of the Reykjanes Ridge.

Key words: earthquake sequences, long-term observations, mid-ocean ridges, seismicity.

1 INTRODUCTION

The Reykjanes Ridge, which extends between the southwesternmost tip of Iceland to the Bight Fracture Zone (located near 56°40′N), is a distinctive section of the Mid-Atlantic Ridge (MAR). This specificity results both from (1) the proximity of the Iceland hotspot, which bears a strong influence on the thermal regime of the upper mantle and crust and on the crustal accretion mechanisms (Magde & Smith 1995; Smith *et al.* 1995; Gardiner *et al.* 2002) and from (2) the obliquity between the Ridge’s general southwesterly trend and the more northerly direction of the individual active volcanic ridges observed along the ridge axis (Applegate & Shor 1994; Searle *et al.* 1998; Tuckwell *et al.* 1998).

The shallow (<1000 m) portion of the Reykjanes Ridge, which lies closest to Iceland, appears to be the location of active magmatic processes. In particular, very recent lava flows were observed along

this ridge near 59.8°N during submersible dives (Shor *et al.* 1990; Crane *et al.* 1997) close to an area where intense seismic activity had been monitored by an airborne sonobuoy deployment (Nishimura *et al.* 1989). These observations suggest that notable magmatic activity takes place along this section of the Reykjanes Ridge, possibly more intense than is observed along other slow-spreading/cold spreading centres. On the other hand, seismic events have been recorded from the Reykjanes Ridge on global, land-based seismic stations and were interpreted as being of tectonic origin (Bergman & Solomon 1990). A recent, short-duration OBS experiment on the Reykjanes Ridge (Mochizuki *et al.* 2000) recorded brief periods of intense micro-seismicity that were also thought to be tectonic. This experiment was, however, located fairly close to Iceland on a shallow (<700 m) portion of the ridge. Thus, in spite of the fact that the spatial and temporal distributions of the seismicity would allow important insights on the magmatic and tectonic processes that are

active along this section of the ridge system, the small-magnitude seismicity of the deepest part (>2000 m) of the Reykjanes Ridge remained largely unknown.

This paper describes in detail four of the five earthquake sequences that were observed along the Reykjanes Ridge by the ‘SIRENA array’ of six autonomous hydrophones during its recent 16-month deployment in the North Atlantic. The SIRENA hydrophones were moored in the sound fixing and ranging (SOFAR) channel, north of the Azores Plateau on the flanks of the Mid-Atlantic Ridge between latitudes 40° 20'N and 50° 30'N. The SIRENA deployment took place in the framework of a France–USA–Portugal co-operative experiment. The *R/V Le Suroit* moored the six instruments during the SIRENA cruise, which sailed from Ponta Delgada (Azores) to Brest from 2002 May 17 to 2002 June 3. The array was recovered during the SIRENA 2/D274 cruise aboard the *RRS Discovery* between Govan (Scotland) and Ponta Delgada (2003 September 12 to 2003 October 1) (the SIRENA Team, 2004).

2 REYKJANES RIDGE EARTHQUAKE SEQUENCES

Earthquakes occurring within oceanic areas generate both seismic phases that travel within the ocean lithosphere and an acoustic phase that propagates in the ocean–water column along the SOFAR channel. This ocean phase results from the conversion of seismic to acoustic waves at the crust/water seafloor interface. The SOFAR channel is a low-velocity zone in the water column, typically located at depths from 700 to 1000 m in the North Atlantic Ocean, which acts as a wave-guide, trapping the acoustic signals. The acoustic phase is referred to as the Tertiary (T-) phase since it has a lower velocity ($\sim 1.5 \text{ km s}^{-1}$, the speed of sound in ocean water) than crustal seismic phases and thus arrives third on land seismic stations, after the compressional (*P*) and shear (*S*) arrivals. Earthquake T-phase arrivals recorded on SOFAR hydrophones have been used successfully for many years to characterize mid-ocean ridge volcanic and tectonic activity (e.g. Dziak *et al.* 1995; Bohnenstiehl *et al.* 2002). Although seismic waves traveling within the solid earth are attenuated rapidly, acoustic waves within the SOFAR channel can travel for very long distances undergoing very little attenuation. This allows for the detection of smaller (and more numerous) mid-ocean ridge earthquakes, relative to traditional seismic monitoring (e.g. Dziak *et al.* 2004a).

Previous work along the 15° to 35°N section of the Mid-Atlantic Ridge has shown that using autonomous hydrophones to detect earthquakes can lower the detection threshold of events from the 4.6 m_b of global seismic networks to 3.0 m_b (Dziak *et al.* 2004a), leading to a 20-fold increase in the number of events detected.

The analysis of the acoustic signals recorded by the SIRENA array from 2002 May to 2003 September led to the localization of 809 earthquakes along the axis of the Reykjanes Ridge (Fig. 1). These events occurred within five individual earthquake sequences. This was rather fortunate as only 22 sequences (defined as more than five spatially clustered earthquakes occurring during a 4 to 48 hr period) were detected along the Reykjanes Ridge by land-seismic networks since 1973 (National Earthquake Information Centre, online catalogue 2004).

The details of the five sequences are: (1) 304 events (beginning 2002 October 6, average location $\sim 58.26^\circ\text{N}$, $\sim 31.80^\circ\text{W}$); (2) 31 events (beginning 2003 January 27, average location $\sim 59.55^\circ\text{N}$,

$\sim 30.23^\circ\text{W}$); (3) 257 events (beginning 2003 February 1, average location $\sim 57.30^\circ\text{N}$, $\sim 33.13^\circ\text{W}$) (4) 182 events (beginning 2003 July 9, average location $\sim 58.08^\circ\text{N}$, $\sim 32.00^\circ\text{W}$) and (5) 35 events (beginning 2003 July 19, average location $\sim 60.89^\circ\text{N}$, $\sim 26.91^\circ\text{W}$). The present work will concentrate on the interpretation of the time distribution of four of these five sequences, as the least numerous events from the 2003 January 27 sequence were also the least accurately located. Our data set gives unique information on the space and time distributions of the seismicity along the slow, hotspot-influenced Reykjanes spreading centre.

The earthquakes detected by the SIRENA array were located using a non-linear least-squares regression algorithm that minimizes the difference between observed and predicted arrival times using standard ocean sound-speed models (Fox *et al.* 2001). The location algorithm is well tested and earthquakes within the hydrophone network typically have location errors of ± 2 km in latitude and longitude at the 68 per cent confidence level. The Reykjanes Ridge, however, is located well outside of the SIRENA network, ~ 800 km north of the northernmost hydrophones. The resulting latitude error is therefore understandably high since there are no hydrophones north of the Reykjanes Ridge, which has the effect of distributing the event locations along great-circle arcs parallel to the north–south elongation of the array. Since the Reykjanes Ridge is within the longitudinal aperture of the array, however, the longitude errors of the sequence events are much smaller (see example on Fig. 2 for the 2002 October 6 sequence). Monte Carlo simulations indicate that the contributions from errors on propagation time within the SOFAR channel to the ‘total’ earthquake location errors are of the order of ± 30 km in latitude and ± 7 km in longitude. Propagation errors, therefore, represent only about half the total uncertainty in epicentre location (the other half being due to arrival-time picking errors and to the distance between the epicentres and the seismic/acoustic conversion points at the seafloor, which is the location given by the inversion process). Since the event location longitude is relatively well constrained, we can be confident in interpreting the earthquake spatial distribution as representing distinct earthquake sequences (Fig. 1 and Table 1). Finally, since the event locations follow a Gaussian latitudinal distribution along the great-circle arc that is fitted through each sequence (Figs 3a and b), the mean locations computed for each sequence likely represent the true source location. As can be seen in Fig. 4, the mean locations for each sequence are either on the Reykjanes Ridge or very near the Reykjanes Ridge axis. When overlain on topographic and structural maps of the axis (Applegate & Shor 1994) (see inserts on Fig. 4), the spatio-temporal distribution of the sequences indicates the Reykjanes Ridge undergoes both tectonic and volcanic rifting episodes that, although separated by months to years, can occur along adjacent sections of the ridge.

The difference in detection levels between land-based seismic arrays and hydrophone arrays moored in the SOFAR channel is illustrated by the relative paucity of earthquakes detected (15 out of 304) from the 2002 October 6 sequence by land-seismic networks. Since only the largest main- and aftershocks are recorded by the seismic networks, these latter observations provide little information on the dynamics of the earthquake sequences. On the other hand, the magnitude–time distribution of the earthquake sequences, as observed by the hydrophones, provides a first insight on the diverse characters of the sequences.

The 2002 October 6 sequence, Figs 5(a) and 6(a1), was initiated by a large normal faulting earthquake (5.6 Mw) followed by a series of smaller aftershocks over the initial 1.5 d. Subsequent to this activity, however, large earthquakes occurred at 1.6 (5.2 m_b) and

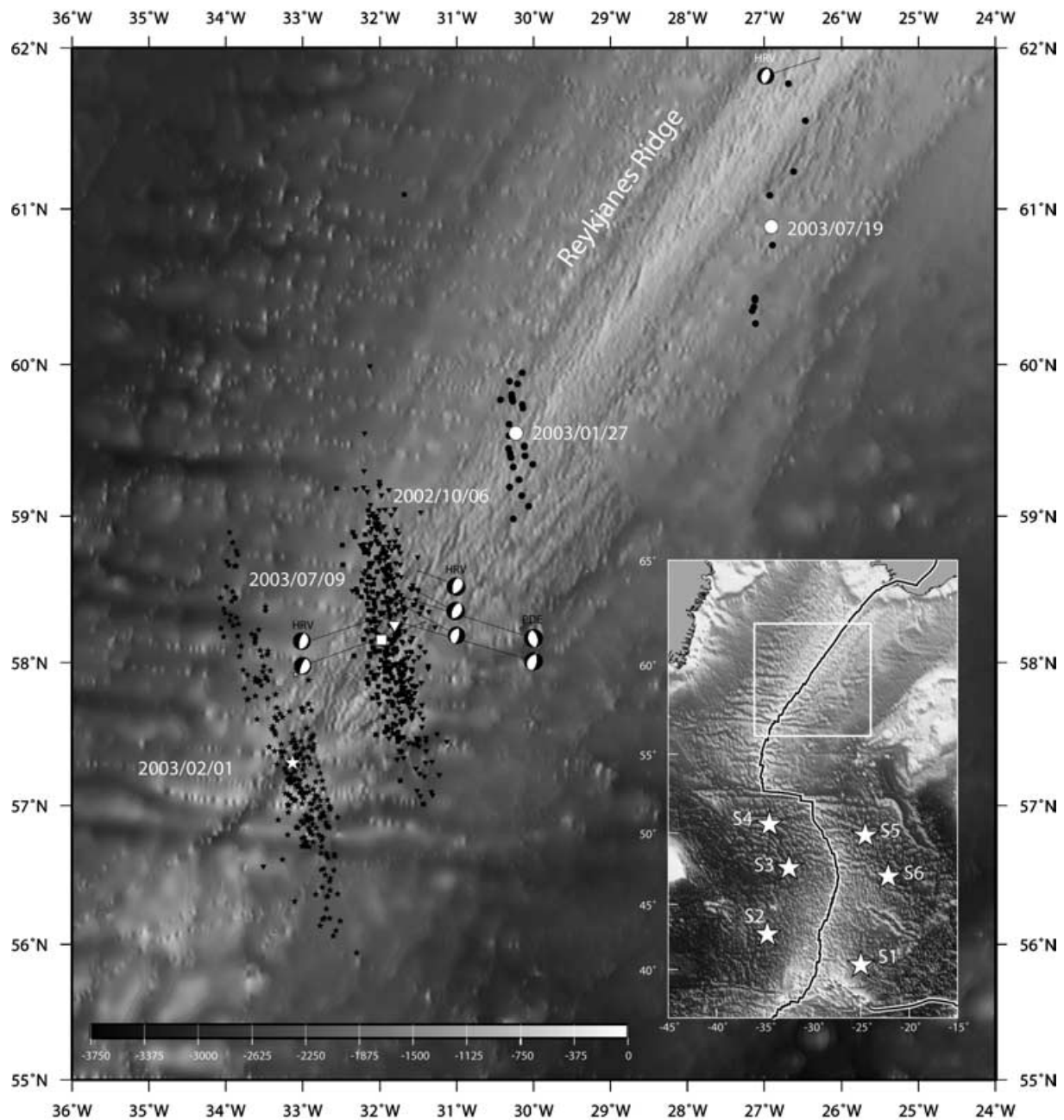


Figure 1. Earthquake locations determined from the acoustic signals recorded on the SIRENA network during the period of operation of the network (from 2002 June to 2003 September). Topography background is from the Ridge Multibeam Bathymetry Synthesis (<http://www.marine-geo.org/ridgebathy/>) over the axial domain of the Reykjanes Ridge and from the predicted topography of Smith & Sandwell (1997) for the rest of the map. Various symbols show events within five individual earthquake sequences. Open corresponding larger symbols show the location of the average position for each sequence. Focal mechanisms are from the Harvard CMT catalogue.

1.8 d (5.7 M_w) into the sequence, and in total the sequence produces five events (out of the 15 reported by the NEIC) within one magnitude unit of the initial event. The 2003 February 1 (Figs 5b and 6b) sequence was initiated by a moderate size (4.4 m_b) earthquake with a slightly larger event (4.8 m_b) occurring less than 2 min later. Three larger events of magnitude 5.6, 5.4 and 5.0 occur at 0.13, 0.23 and 1.07 d into the sequence.

In contrast to the 2002 October 6 sequence, the 2003 July 9 sequence was initiated by moderate-size earthquake ($\sim < 4.0 m_b$) that was followed by nine NEIC-located events occurring during a brief period of 0.35 d. The magnitude–time distribution shows a series

of small events that vary in magnitude through time (Fig. 5c). The 2003 July 19 sequence (Figs 5d and 6d) was initiated by a 4.5 m_b earthquake that was followed by 10 additional NEIC-located events during the next 0.37 d.

In summary, with the exception of the 2002 October 6 sequence, all sequences are very short and end very abruptly. Such observations are consistent with the sequences being magmatic, where rate–state friction predicts that the duration of aftershocks effects (related to the large magnitude events within the swarm) will be shortened or suppressed as the stressing rate increases associated with dike/magma movement (e.g. Toda *et al.* 2002).

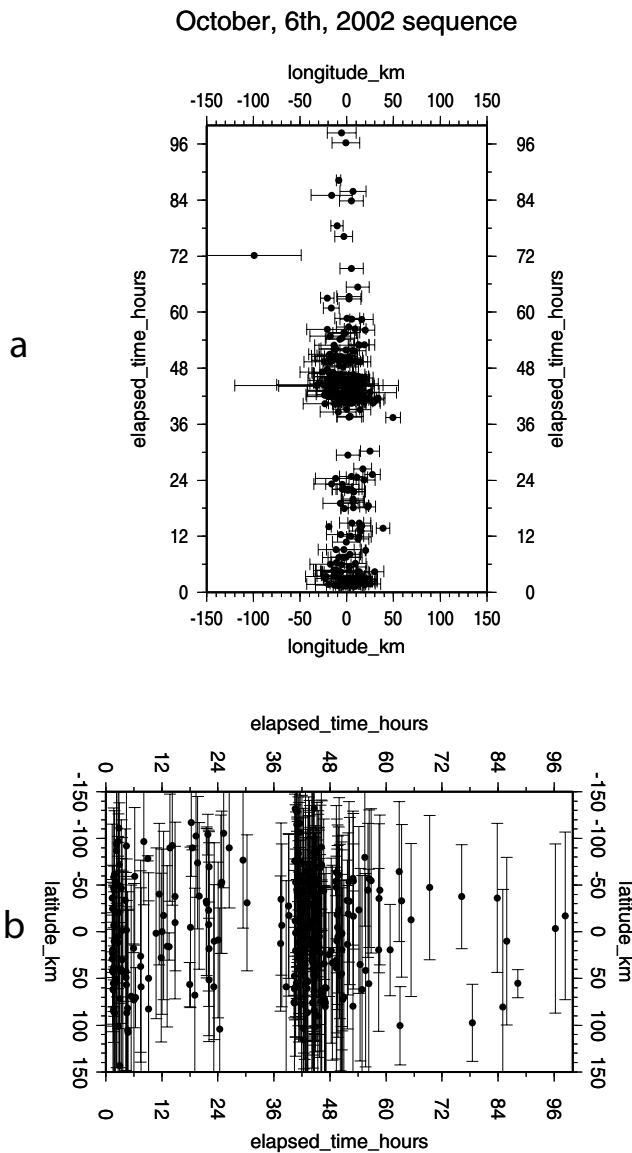


Figure 2. Longitudinal (2a) and latitudinal (2b) distributions versus elapsed time of the events within the 2002 October 6 sequence. The origin of times is arbitrarily fixed at the time of the teleseismic initial event. Origins of distances are taken at the average epicentre location for the sequence (58° 15.6'N; -31° 48'W).

3 TIME DISTRIBUTION OF THE REYKJANES RIDGE EARTHQUAKE SEQUENCES

One common measure of the magmatic or tectonic character of earthquake sequences is the goodness-of-fit of the event rate versus

time distribution to a modified Omori law (or MOL) model of aftershock decay (e.g. Utsu *et al.* 1995; Wennerberg & Sharp 1997; Bohnenstiehl *et al.* 2002). Fig. 6 shows the cumulate number of seismic events versus time for the 2002 October 6, 2003 February 1, 2003 July 9 and 19 earthquake sequences. The time-axis origin is the time of the first NEIC-recorded event, which would be considered as the mainshock in the case of a tectonic sequence. Prior to analysing the time–rate data, the hydroacoustic earthquake catalogue is filtered to include only events with source levels (acoustic magnitudes) estimated to be ~178 dB (~175 dB for the July 2003 sequence). At smaller acoustic magnitudes, the source level–frequency data can be seen to depart from its characteristic power-law distribution (e.g. Bohnenstiehl *et al.* 2002; Dziak *et al.* 2004a), indicating the failure of the array to properly record the smaller earthquakes in the population. It should be noted that the levels of the acoustic signals recorded by the autonomous hydrophones (such as, for example those shown on Figs 5a–d) should not be viewed as representing absolute magnitudes of the earthquakes but should be considered as relative values. These acoustic levels indeed depend on many factors, among which are the sensor response characteristics, the attenuation laws in the SOFAR channel and, last but not the least, the efficiency of the seismic to acoustic signal conversion at the seafloor interface. ‘Absolute’ magnitudes can possibly be obtained after adjusting a linear fit through a set of m_b versus SL points for the larger teleseismic events whose magnitude was determined by land-based networks. Caution, however, should be exercised when using this linear law to estimate the size of small- to moderate-magnitude earthquakes that are recorded only on the hydrophone array.

The sequence beginning 2002 October 6 was initiated by a 5.6 Mw earthquake and the rate of activity in the first part of the sequence is adequately fit by a MOL model Fig. 6(a1). When data from the first 0.75 d of the sequence are fitted (Fig. 6(a2)), the decay constant (p-value) is found to be 1.01 ± 0.25 (1-sigma error), somewhat lower than was estimated for two sequences south of the Azores by Bohnenstiehl *et al.* (2002), but within the range of values reported in the literature (Utsu *et al.* 1995). An abrupt increase in event rate, at ~1.6 d after the first 5.5 Mw event, follows a 5.2 Mw event, this being also generally consistent with mainshock-aftershock activity. A 5.6 Mw event is observed but a few hours later. Most of the subsequent rate increases would be tied to these two large magnitude earthquakes, but also depend, at any time, on the aftershock seismicity rate just beforehand (Toda & Stein 2003). In short, even if some magmatic influence cannot be totally ruled out (as would, for example result in the event rate increase at about 2.2 d after the first main event, which is not preceded by any teleseismic large event), a large part the observed 2002 October 6 sequence is consistent with tectonic activity.

Conversely, the 2003 February 1 (Fig. 6b), 9 and 19 July 2003 (Figs 6c and 6d) sequences can neither be described adequately by an MOL curve nor, as could be the case for the 2002

Table 1. Time and space characteristics of five earthquake sequences observed along the Reykjanes Ridge during the deployment of the SIRENA autonomous hydrophone array.

Date of sequence	Start time(GMT)	No. of events	Average latitude	Average longitude	Mean lat. error	Mean long. error
2002 October 6	01:18	304	58° 15.6'N	-31° 48'W	0.743° ~ 82 km	0.236° ~ 14 km
2003 January 27	05:20	31	59° 33.1'N	-30° 13.6'W	0.638° ~ 71 km	0.082° ~ 5 km
2003 February 1	15:44	257	57° 20'N	-33° 7.8'W	0.696° ~ 77 km	0.361° ~ 22 km
2003 July 9	08:22	182	58° 4.8'N	-32° 0'W	0.394° ~ 44 km	0.132° ~ 8 km
2003 July 19	13:12	35	60° 53.4'N	-26° 54.6'W	0.798° ~ 88 km	0.273° ~ 15 km

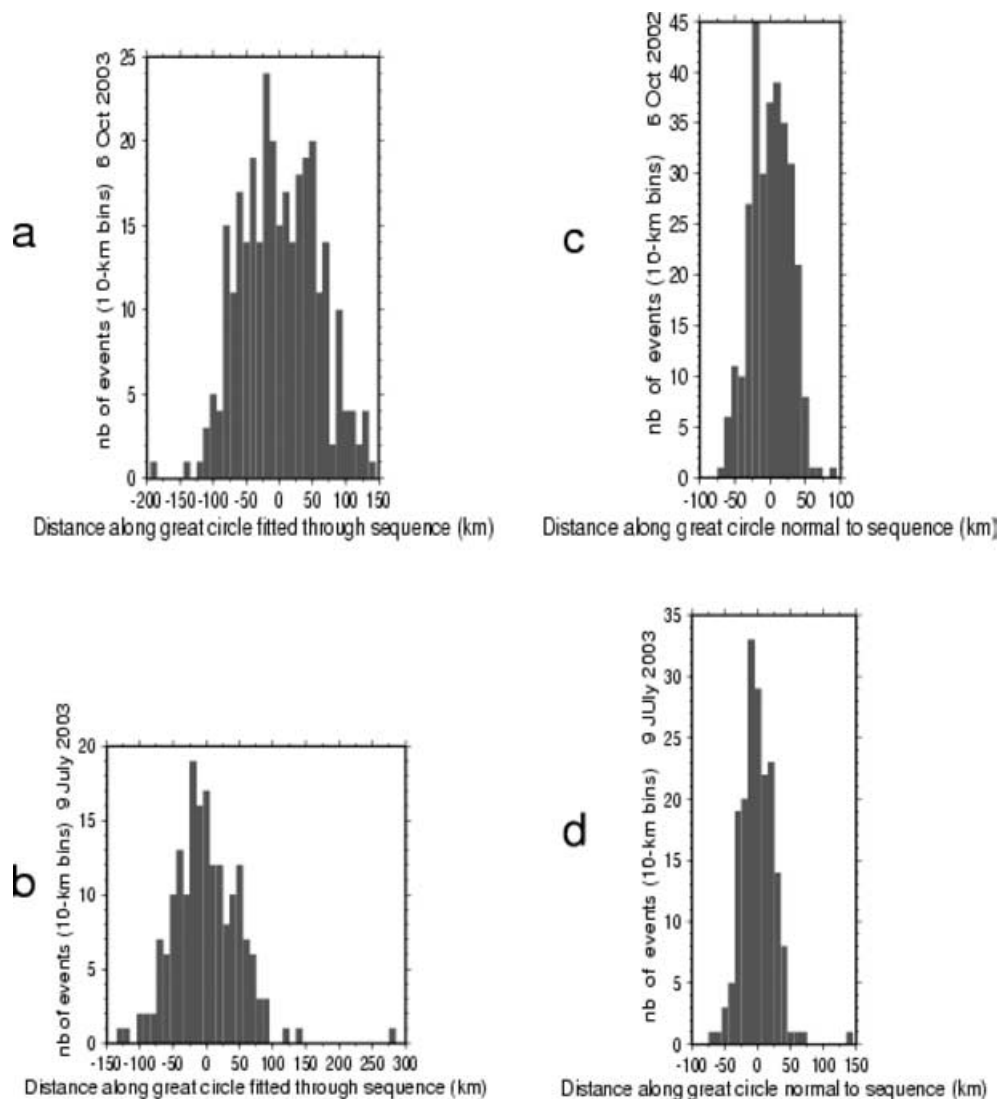


Figure 3. Histograms of the number of events plotted as functions: (1) of distances along a great circle fitted through the locations of epicentres in the 2002 October 6 sequence (3a) and in the 2003 July 9 sequence (3c); (2) of distances along great circles normal to the best-fitting circles (3b and d). The origin of distances is arbitrarily fixed at the average epicentre location of each sequence.

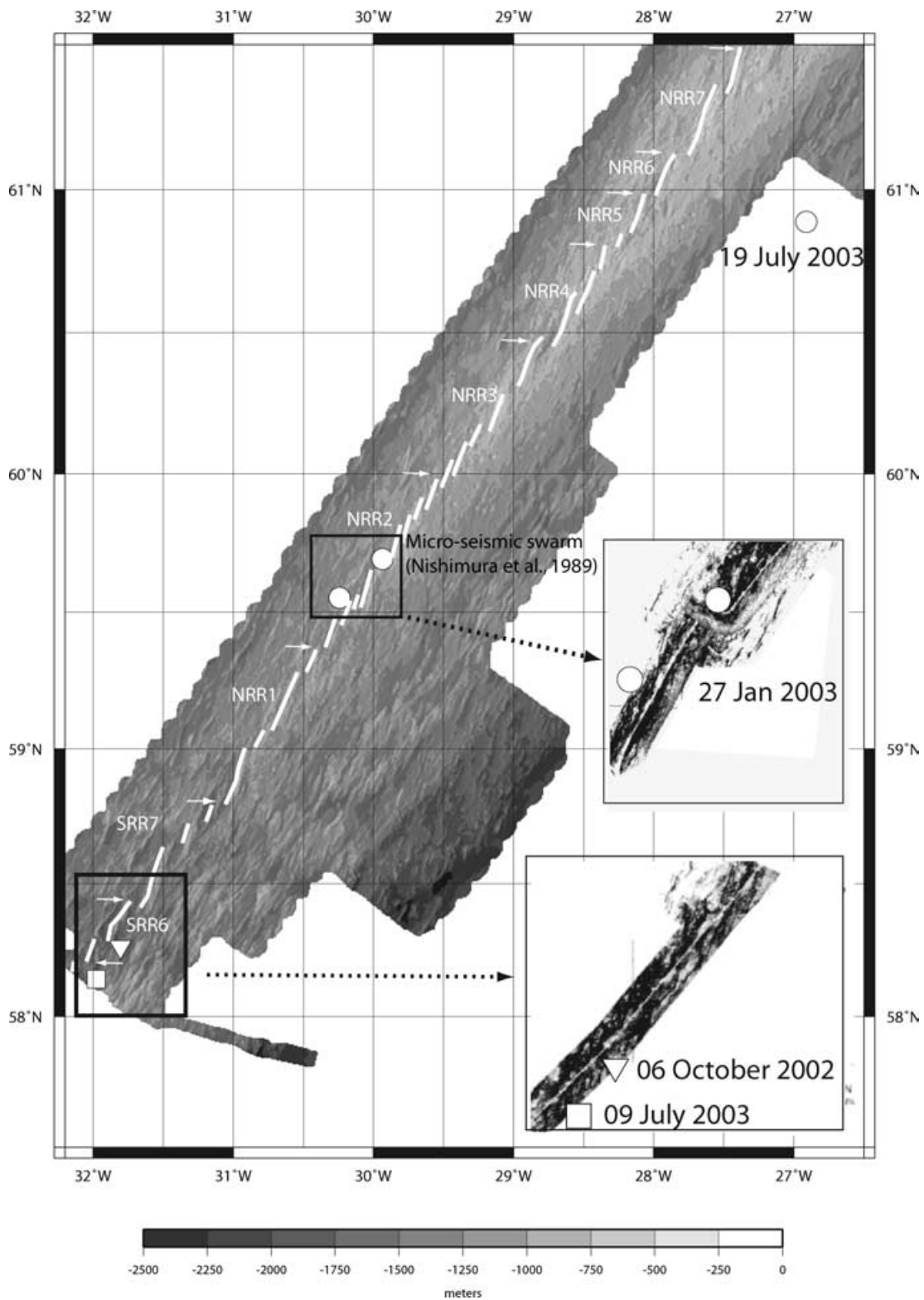
October 6 sequence, by a ‘nested MOL’ curve (e.g. Utsu *et al.* 1995). In fact, the standard maximum likelihood routines used in these analyses (e.g. Ogata 1983) fail to provide a solution, reflecting both the poor fit of the data to this model and the short duration of the sequences. Moreover, for the 2003 July 9 sequence, the total number of hydroacoustically detected events is larger than expected for aftershock activity, given the magnitude of the largest event ($5.1 m_b$) (cf. Bohnenstiehl *et al.* 2002). The rate of activity within these sequences could be more consistent with a magmatic triggering mechanism rather than with an initiation by a tectonic mainshock. However, the level of seismicity in the Reykjanes Ridge sequences is one order of magnitude lower than observations at the CoAxial segment at the intermediate-spreading rate Juan de Fuca Ridge during a dike emplacement and subsequent eruption (Dziak *et al.* 1995). On the other hand, compared to the 2001 March Lucky Strike earthquake swarm on the MAR, which was associated with a possible dike emplacement episode (Dziak *et al.* 2004b), the two other sequences which may also be from magmatic triggering along the Reykjanes Ridge (2003 February 1 and 2003 July 9) have about

twice as many events as the Lucky Strike swarm. Seismicity rates are similar, reaching peaks between 32 and 38 events hr^{-1} for the larger sequences compared to the 42 events hr^{-1} at Lucky Strike, although the rise towards peak activity and the subsequent decay rates in each sequence are less drastic than the Lucky Strike swarm.

4 DISCUSSION AND CONCLUSIONS

The 16-month deployment of the SIRENA hydrophone array in 2002–2003 resulted in the detection of a surprisingly large number (5) of earthquake sequences along the Reykjanes Ridge south of Iceland. The sequences were initiated by moderate-to-large magnitude earthquakes, with at least one exhibiting an Omori-like decay rate in the early part of the sequence. However, none of them can be completely described as a simple mainshock-aftershock sequence.

Whereas the power-law decay rate of an aftershock sequence reflects the process of stress relaxation following a large magnitude earthquake, most earthquake swarms (sequences that lack a dominant mainshock earthquake) are thought to be driven by



Downloaded from https://academic.oup.com/gji/article/162/2/516/553338 by guest on 19 February 2021

Figure 4. Average epicentre locations of four earthquake sequences localized with respect to the axial structure of the Reykjanes Ridge, overlain on the topography background from the Ridge Multibeam Bathymetry Synthesis (<http://www.marine-geo.org/ridgebathy/>). Symbols showing the average locations of four of the five sequences are the same as are those used in Fig. 1 (no detailed multibeam bathymetry is available around the average location of the the 2003 February 1 sequence). The location of a microseismic swarm (Nishimura *et al.* 1989) is also shown. Inserts show the average location of three sequences and of the microseismic swarm over the SeaMARC II side scan sonar imagery published by Applegate & Shor (1994).

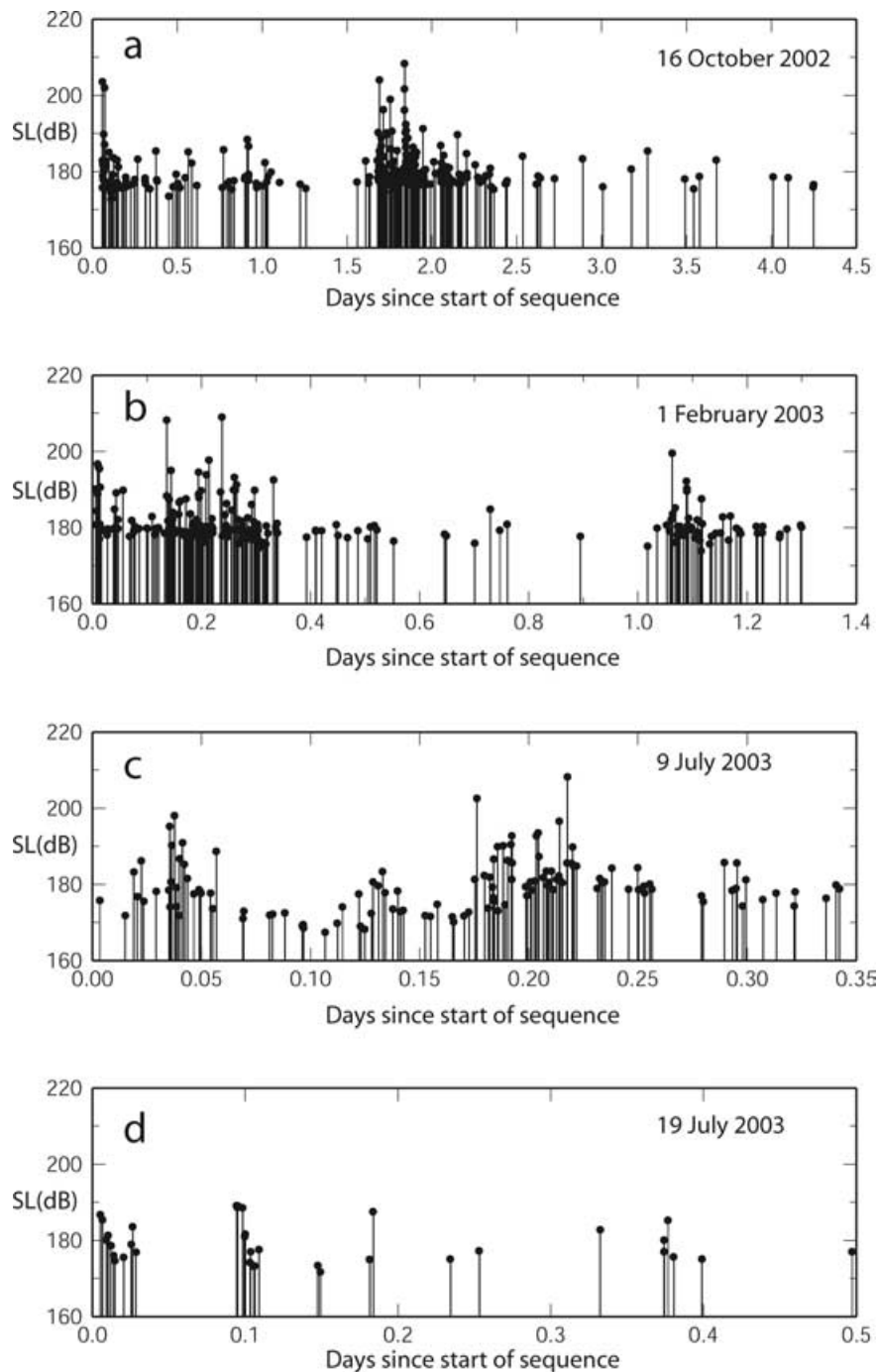


Figure 5. Acoustic amplitudes SL (in dB, i.e. $1 \mu\text{Pa}$) versus time for the 2002 October 6 (5a), 2003 February 1 (5b), 2003 July 9 (5c) and 2003 July 19 (5d) sequences observed on the Reykjanes Ridge. The origin of time is fixed arbitrarily for each sequence at the time of the teleseismic initial event.

magmatic processes or pore-fluid movements within the crust (e.g. Hill 1977; Spicak 2000). Consequently, although the moderate-to-large magnitude events that initiated the Reykjanes sequences may be manifestations of stretching associated with the divergence of tectonic plates, their swarm-like nature suggests interaction with magma and/or magma-derived hydrothermal fluids. Conceivably, these short-duration sequences may involve the rupturing of hydrothermal seals following an initial tectonic event—allowing fluids to migrate into and reduce the strength of existing fault zones—rather than triggering in direct response to magma movement.

ACKNOWLEDGMENT

Funding from various sources made the SIRENA experiment possible: the cost of ship time for both cruises was provided by the French Ministry of Research. We thank the masters and crews of the *R/V Le Suroit* and *RRS Discovery* for their help and seamanship. We are extremely grateful to A. Lau and H. Matsumoto for their efforts in software and hardware development, respectively, and M. Fowler for his skilled work at sea. The development, building and deployment of the autonomous hydrophones during the SIRENA experiment

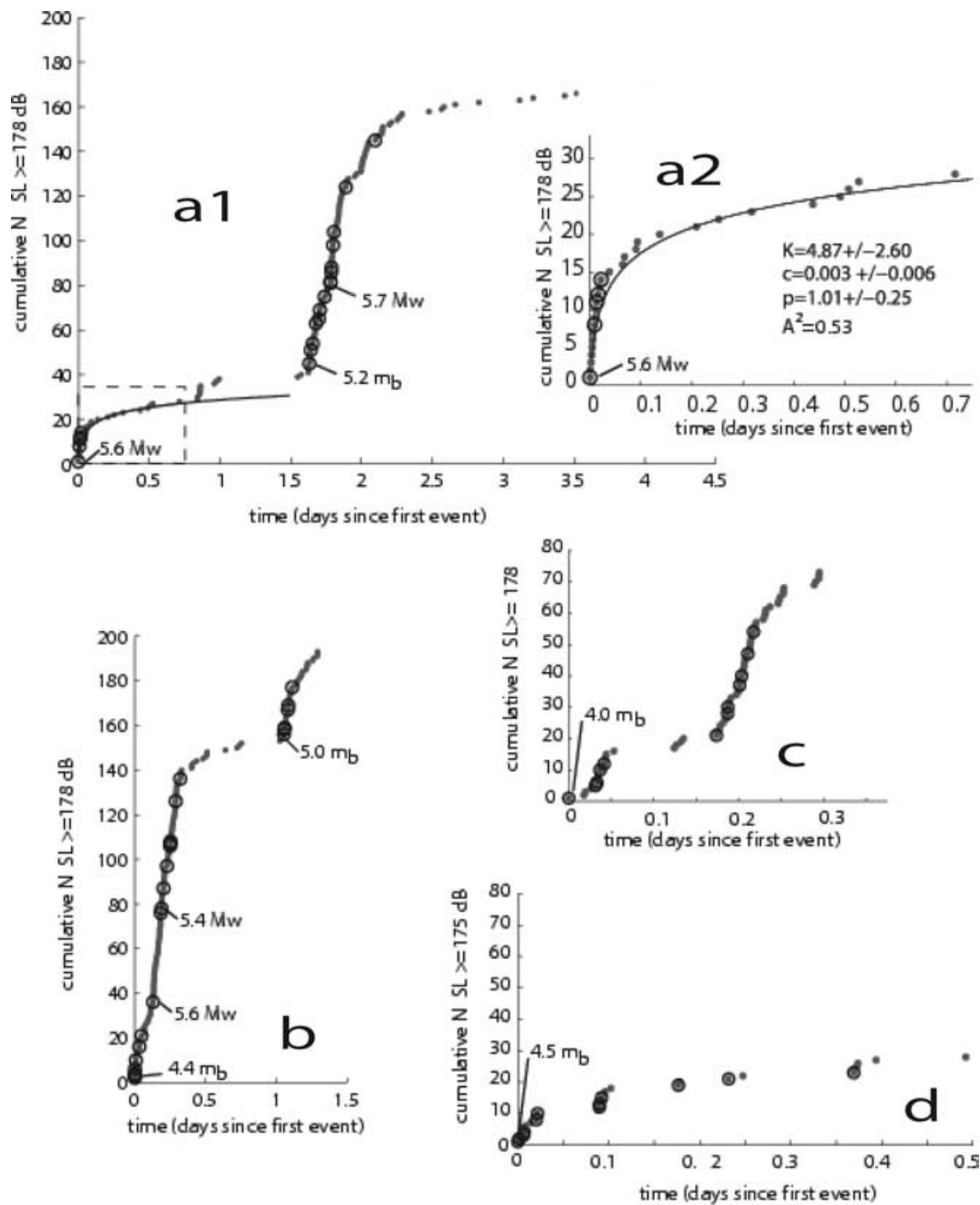


Figure 6. Cumulated number of events versus time for the 2002 October 6 [6a], 2003 Feb 1 [6b], July 9 [6c] and 2003 July 19 [6d] event sequences, as derived from the hydrophone records. Events of sufficient size to be listed in the *Reviewed Event Bulletin* of the IDC and NEIC catalogue are indicated by open circles (all NEIC events are also listed in the IDC). Fig. 6(a2) shows a blow-up of the initial 1.5 d of the 2002 October 6, sequence shown in Fig. 6(a1). In Figs 6(a1) and 6(a2), a Modified Omori Law fitting the initial 0.75 d of the October 6 sequence is also shown. The parameters associated with this law (K , c and p) and the Anderson–Darling goodness-of-fit parameter A^2 are listed in Fig. 6(a2) (values of $A^2 < 1$ indicate that the decay rate is adequately fitted by the MOL model; Bohnstiehl *et al.* 2002).

were provided by the NOAA Ocean Exploration Programme. Deployment and analysis of the south Azores hydrophone array was made possible by support from the U.S. National Science Foundation (grants OCE-9811575, OCE-0137164 and OCE-0201692). Salaries and travel costs were provided to their nationals by the three countries involved. The Portuguese members of the team would like to acknowledge the support of the STAMINA project (POCTI/MAR). Data interpretation which is the base of this paper was conducted

while R. Dziak stayed in Brest as an invited professor by the Université de Bretagne Occidentale and N. Lourenço benefited from a travel grant in the framework of the IFREMER-ICCT 2003 cooperation programme in oceanology. We thank Dr T. Minshull, GJI Editor, Dr Barclay and an anonymous referee, for their careful and constructive reviews of the first version of this paper. This paper is IUEM contribution number 943, PMEL contribution number 2800 and LDEO contribution number 6755.

REFERENCES

- Applegate, B. & Shor, A.N., 1994. The northern Mid-Atlantic and Reykjanes Ridges: spreading center morphology between 55°50'N and 63°00'N, *J. geophys. Res.*, **99**, 17 935–17 956.
- Bergman, E.A. & Solomon, S.C., 1990. Earthquake swarms on the Mid-Atlantic Ridge: products of magmatism or extensional tectonics? *J. geophys. Res.*, **95**, 4943–4965.
- Bird, P., 2003. An updated digital model of plate boundaries, *Geochemistry, Geophysics Geosystems*, **4**(3), 1027, doi:10.1029/2001GC000252.
- Bohnstiehl, D.R., Tolstoy, M., Dziak, R.P., Fox, C.G. & Smith, D.K., 2002. Aftershock sequences in the mid-ocean ridge environment: an analysis using hydroacoustic data, *Tectonophysics*, **354**, 49–70.
- Crane, K., Johnson, L., Applegate, B., Nishimura, C., Buck, R., Jones, C., Vogt, P. & Kos'yan, R., 1997. Volcanic and seismic swarm events on the Reykjanes Ridge and their similarities to events on Iceland: results of a rapid response mission. *Mar. geophys. Res.*, **19**, 319–338.
- Dziak, R.P., Fox, C.G. & Schreiner, A.E., 1995. The June–July 1993 Seismo-acoustic event at CoAxial Segment, Juan de Fuca Ridge: evidence for a lateral dike injection, *Geophys. Res. Lett.*, **22**, 135–138.
- Dziak, R.P., Bohnstiehl, D.R., Matsumoto, H., Fox, C.G., Smith, D.K., Tolstoy, M., Lau, T.-K., Haxel, J.H. & Fowler, M.J., 2004a. P- and T-wave Detection Thresholds, Pn Velocity Estimate, and Detection of Lower Mantle and Core P-waves on Ocean Sound-Channel Hydrophones at the Mid-Atlantic Ridge, *Bull. Seis. Soc. Am.*, **95**, 665–677.
- Dziak, R.P. *et al.*, 2004b. Long-term monitoring of Mid-Atlantic Ridge earthquake activity using autonomous hydrophone arrays. *Ridge 2000 Mid-Atlantic Ridge Workshop*. Providence RI, 1–2 March. <http://ridge2000.bio.psu.edu/NewR2kSite/mw/MeetingArchives/MARWorkshop/MAR-abstracts.php>
- Fox, C.G., Matsumoto, H. & Lau, T.-K., 2001. Monitoring Pacific Ocean seismicity from an autonomous hydrophone Array, *J. geophys. Res.*, **106**, 4183–4206.
- Gardiner, A., Peirce, C., Searle, R. & Sinha, M., 2002. Cyclicity of crustal accretion at the Reykjanes Ridge, *EOS Trans. AGU*, **83**, 1355.
- Hill, D.P., 1977. A model for earthquake swarms, *J. geophys. Res.*, **82**, 1347–1352.
- Magde, L.S. & Smith, D.K., 1995. Seamount volcanism at the Reykjanes Ridge: relationship to the Iceland hotspot. *J. geophys. Res.*, **100**(B5), 8449–8468.
- Mochizuki, M., Brandsdottir, B., Shiobara, H., Gudmundsson, G., Stefanson, R. & Shimamura, H., 2000. Detailed distribution of microearthquakes along the northern Reykjanes Ridge, off SW-Iceland. *Geophys. Res. Lett.*, **27**, 1945–1948.
- Nishimura, C.E., Vogt, P.R., Smith, L. & Boyd, J.D., 1989. Investigation of a possible underwater volcanic eruption on the Reykjanes Ridge by airborne sonobuoys and AXBT's. *EOS Trans. AGU*, **70**, 1301.
- Ogata, Y., 1983. Estimation of the parameters in the modified Omori formula for aftershock frequencies by the maximum likelihood procedure, *J. Phys. Earth*, **31**, 115–124.
- Searle, R.C., Keaton, J.A., Owens, R.B., White, R.S., Meckleburg, R., Parsons, B. & Lee, S.M., 1998. The Reykjanes Ridge: structure and tectonics of a hot-spot-influenced, slow-spreading ridge from multibeam bathymetry, gravity and magnetic investigations. *Earth Planet. Sci. Lett.*, **160**, 463–478.
- Spicak, A., 2000. Earthquake swarms and accompanying phenomena in intraplate regions: a review. *Studia geoph. et geod.*, **44**, 89–106.
- Shor, A.N., Nishimura, C.E., Czarnecki, M. & Vogt, P.R., 1990. Lava extrusion from the 1989 reykjanes Ridge seismic swarm? Probably yes (Sea-MarII). *EOS Trans. AGU*, **71**, 1602.
- Smith, W.H.F. & Sandwell, D.T., 1997. Global sea floor topography from satellite altimetry and ship depth soundings, *Science*, **277**, 1956–1962.
- Smith, D.K., Humphris, S.E. & Bryan, W.B., 1995. A comparison of eruptive units at the Reykjanes Ridge and the Mid-Atlantic Ridge, 24–30N, *J. geophys. Res.*, **100**, 22 485–22 498.
- The SIRENA team*: Goslin, J., Perrot, J., Royer, J.-Y., Martin, C., Fox, C.G., Dziak, R.P., Matsumoto, H., Fowler, M.J., Haxel, J.H., Luis, J., Lourenço, N. & Bazin, S., 2004. Interactions between the MAR and the Azores hotspot as imaged by seismicity distributions using autonomous hydrophone arrays. *Workshop on 'Seismo-acoustic Applications in Marine Geology and Geophysics'*. Woods Hole OI, 24–26. March, 2004.
- Toda, S., Stein, R.S. & Sagiya, T., 2002. Evidence from the AD 2000 Izu Islands swarm that stressing rate governs seismicity, *Nature*, **419**, 58–61.
- Toda, S. & Stein, R.S., 2003. Toggling of seismicity by the 1997 Kagoshima earthquake couplet: a demonstration of time-dependent stress transfer, *J. geophys. Res.*, **108**(B12), 2567, doi:10.1029/2003JB002527.
- Tuckwell, G.W., Bull, J.M. & sanderson, D.J., 1998. Numerical models of faulting at oblique spreading centres. *J. geophys. Res.*, **103**(B7), 15 473–15 482.
- Utsu, T., Ogata, Y. & Matsu'ura, R., 1995. The centenary of the Omori formula for a decay law of aftershocks activity, *J. Phys. Earth*, **43**, 1–33.
- Wennerberg, L. & Sharp, R.V., 1997. Bulk-friction modeling of afterslip and the modified Omori law. *Tectonophysics*, **277**, 109–136.